Synthesis, computational studies, inelastic neutron scattering, infrared and Raman spectroscopy of ruthenocene

Stewart F. Parker and Ian R. Butler

Published version information

This is the peer reviewed version of the following article:

SF Parker and IR Butler. 'Synthesis, computational studies, inelastic neutron scattering, infrared and Raman spectroscopy of ruthenocene.' European Journal of Inorganic Chemistry, vol. 2019, no. 8 (2018): 1142-1146.

DOI: 10.1002/ejic.201800914

Synthesis, computational studies, inelastic neutron scattering, infrared and Raman spectroscopy of ruthenocene

Stewart F. Parker,*[a] and Ian R. Butler[b]

Abstract: In this work we report a new and simplified synthesis of ruthenocene that prevents the formation of unwanted by-products. We have also revisited the vibrational spectroscopy of this iconic molecule and in addition to infrared and variable temperature Raman spectra, we present the first inelastic neutron scattering (INS) spectrum, a technique that is little used in inorganic chemistry. The Raman spectra in the low energy range (<200 cm^{-1}) clearly show that the mode assigned as the ring–Ru–ring torsion is a librational mode. By generating the INS spectra predicted by previous assignment schemes, we are able to show that they are all, at least partially, wrong because they fail to correctly predict the experimental INS spectrum. In the case of ruthenocene, the addition of INS data, in combination with periodic-DFT calculations, has enabled the first correct assignment of the internal modes of ruthenocene. This straightforward means to test proposed assignments is one of the great strengths of vibrational spectroscopy with neutrons.

Introduction

The discovery of ferrocene[1] and the recognition[2] of its unprecedented *bis*-η^5 mode of coordination marked the beginning of modern organometallic chemistry. It was very quickly realised[3] that ruthenium and osmium should form analogous compounds and the preparation of *bis*-η^5-cyclopentadienyl ruthenium (ruthenocene[3]) and *bis*-η^5-cyclopentadienyl osmium (osmocene[4]) soon followed.

The vibrational spectroscopy of all three compounds has been characterised, *e.g.*[5] with ferrocene being the most studied. However, the spectroscopy is complicated by selection rules. These are irrelevant for inelastic neutron scattering (INS) spectroscopy,[6] a technique that is little used in inorganic and organometallic chemistry. It has the advantage that, in principle, all the modes are observable. In practice, the spectra are dominated by modes involving hydrogen motion and, for instrumental reasons, the optimal spectral range is 0 – 1600 cm^{-1}.[7] To date, only ferrocene has been investigated by INS spectroscopy.[8]

Literature methods for the synthesis of ruthenocene are complex involving either a Grignard reagent[3] or the preparation of sodium cyclopentadienyl.[9] In this work, we present a new and much simpler synthesis of ruthenocene together with a detailed spectroscopic characterization of the solid state spectra by infrared, Raman and INS spectroscopies. A complete assignment is made *via* periodic density functional theory (periodic-DFT). All previous work has relied on isolated molecule calculations[10] that neglect the effect of the solid state.

Results and Discussion

Synthesis

As mentioned, there are many synthetic routes to ruthenocene which essentially use the reaction of a metal or metalloid cyclopentadienide with a suitable ruthenium (II) or (III) complex.[3,11] When Ru (III) is used, a reducing agent is also required. In our labs the method of choice is one developed in-house in 1981 which is essentially a variant of one of the general published synthetic methods.[12] The method is shown in Scheme 1. This uses hydrated ruthenium trichloride, freshly cracked dicyclopentadiene (to give cyclopentadiene) and powdered zinc, as the reducing agent. The difference of our method is that the reaction is performed in ethanol at low temperature. What is of interest in this synthetic route is that the deep blue color attributed to an initially formed ruthenocenium complex, is discharged rapidly, (< 0.1 s) on warming from -60°C to room temperature to leave a clear solution with only the grey colloidal zinc remaining. Thus, the reduction step is clearly observable. The workup is essentially the same as the method used by Porri *et al*.[12a], which involves crystallization of the colorless iridescent ruthenocene

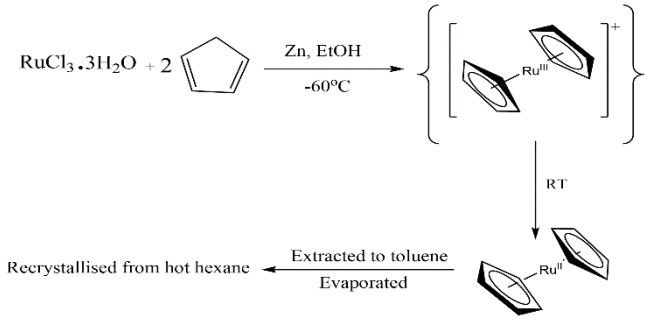

Scheme 1. Synthesis of ruthenocene. The intermediate ruthenocenium ion is not isolated.

from ethanol. By removing the need for heating the solution, unwanted by-products are not formed (see Figures S1 and S2) and yields are higher. The reaction is carried out typically on a 5-10 g scale of ruthenium trichloride trihydrate but is fully scaleable to the ten's of gram scale.

[a] Dr Stewart F. Parker
ISIS Facility
STFC Rutherford Appleton Laboratory
Chilton, Didcot, Oxon OX11 0QX, UK
E-mail: stewart.parker@stfc.ac.uk
[b] Dr Ian. R Butler
School of Chemistry
Bangor University
Bangor, Gwynedd, Wales, LL57 2UW, UK

Supporting information for this article is given via a link at the end of the document.

Vibrational Spectroscopy

Figure 1 shows the infrared, Raman and INS spectra of ruthenocene. The complementarity of the three techniques is readily apparent and emphasizes the need for all three in order to observe all of the modes. Our infrared and Raman data are in complete agreement with that of Adams and Fernando[13] and of Bodenheimer and Low.[14] The INS spectrum has not been previously reported. The complete (0–3200 cm^{-1}) Raman spectra as a function of temperature are shown in Figures S3 and S4 of the Supporting Information.

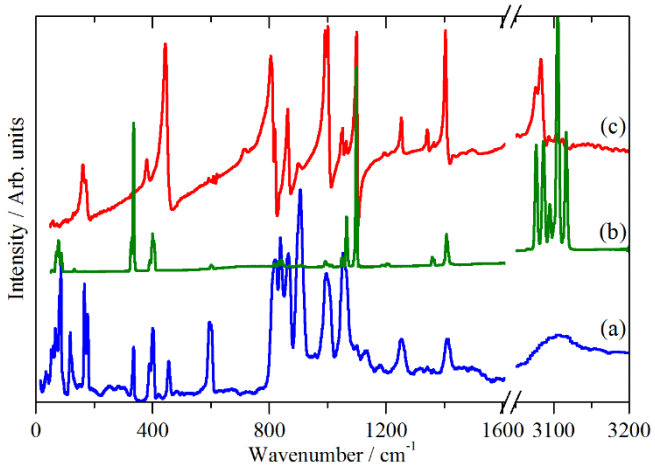

Figure 1. Vibrational spectra of ruthenocene: (a) infrared at room temperature, (b) Raman at 10 K and (c) INS at 10 K.

One of the most problematic modes to assign has been the ring–Ru–ring torsion. This was assigned at 134 cm^{-1},[13,14] although it was recognized that the temperature dependence was anomalous: unlike all the other internal modes this undergoes a marked shift on cooling. The low energy region is shown in detail in Figure 2 and the shift in the mode from 106 cm^{-1} at 300 K to 131 cm^{-1} at 10 K is clearly seen. However, a similar temperature dependence is seen for the lattice modes at 40 – 100 cm^{-1} , consistent with the shrinkage in the unit cell volume[15], (818 $Å^3$ at 300 K and 789 $Å^3$ at 101 K), and we assign the 131 cm^{-1} mode to a libration. The detailed assignment of the internal modes of ruthenocene is considered in the next section.

Assignment of the Spectra

There have been several previous assignments of the vibrational spectra of ruthenocene[5,10,13,14] and these are summarized in columns 4 – 7 of Table 1. It is apparent that there is no consensus between the assignments. Comparison of observed and calculated INS spectra is a very stringent test of an assignment scheme.[6] We have previously shown that while the transition energies are very dependent on the quality of the calculation, the atomic displacements of each atom in the mode are relatively insensitive, so long as the calculated geometry is reasonably correct.[16] This means that the INS spectrum can be simulated by replacing the calculated transition energies with those from the literature on a mode-by-mode basis. Figure 3 shows the results for the literature assignments in Table 3. It can be seen that none of the calculated spectra match the experimental data. All fail to reproduce the very strong feature at ~900 cm^{-1}, this is probably because there are only very weak features at this energy in the Raman and infrared spectra, Figure 1b,c, so were not considered to be fundamentals. In contrast, the intensity in the 1200 cm^{-1} region is overestimated because weak modes in this region were assigned as fundamentals. Figure 1a

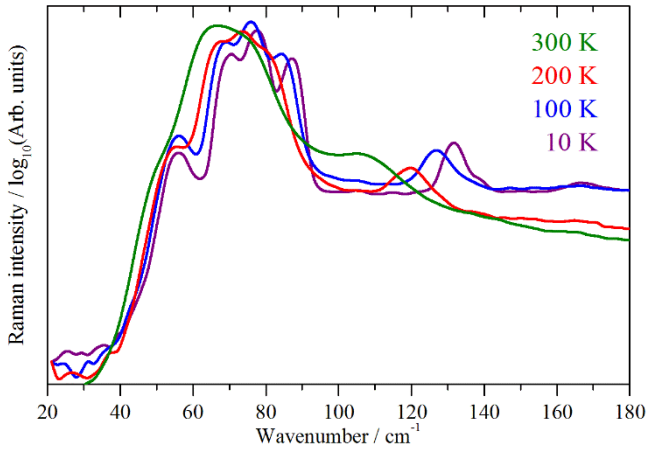

Figure 2. Variable temperature 532 nm Raman spectra of ruthenocene in the low energy region. Note the *y*-axis is logarithmic.

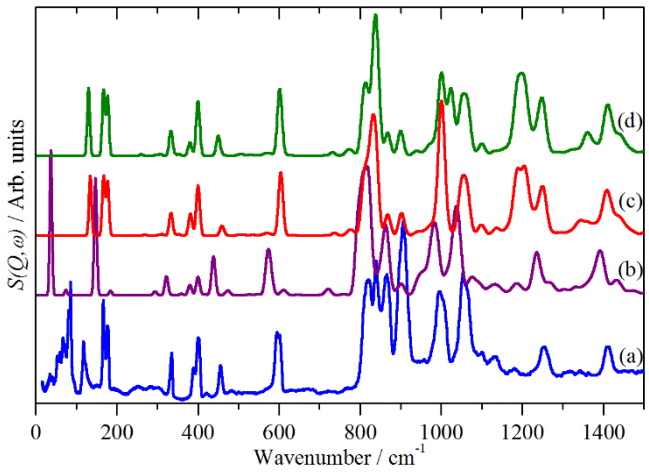

Figure 3. Comparison of INS spectra of ruthenocene: (a) experimental and those calculated from the assignment of (b) Prosenc *et al*,[10a] (c) Adams and Fernando[13] and (d) Bodenheimer and Low[14]

shows that there are only overtones and combinations at this energy. As shown in the previous section, the assignment of the torsional mode to the feature at ~130 cm^{-1} is clearly erroneous.

From Figure 3, it is apparent that assignments based on neither empirical correlations[13,14] or isolated molecule DFT calculations[10a] are able to reproduce the data successfully. To address this problem, we have carried out a periodic-DFT calculation of the complete orthorhombic unit cell, (space group *P*nma[15]). The isolated molecule has D_{5h} symmetry, however, fivefold symmetry is incompatible with long range order and in the crystal, the molecule occupies a site of C_s symmetry. The correlation scheme (reproduced from [14]) is shown in Figure S5 of the Supporting Information. The calculated transition energies for the complete unit cell, together with the mode number and

symmetry of the "parent" mode under D_{5h} symmetry, are given in Table S1 of the Supporting Information. In most cases, the factor group splitting is small, ~10 cm^{-1} or so, the only exception is mode 14, an out-of-plane C–H deformation, which shows a very large splitting of 50 cm^{-1}. We have no explanation for this anomaly.

In Figure 4, we compare the results of the periodic-DFT calculation of the complete orthorhombic unit cell, 4b, with the experimental spectrum, 4a. It is immediately obvious that there is a much better match. The only area of serious disagreement is around 800 cm^{-1}, where a doublet rather a triplet is observed. By slightly shifting the calculated transition energies to match the experimental ones, Figure 4c is obtained. It can be seen that for the internal modes the agreement is almost exact. Column 7 of Table 1 lists the average values of the transitions from Table S1. It can be seen that the "best fit" values of column 8 of Table 1 are in close agreement with those from the periodic-DFT calculation, column 7. Note that column 8 contains experimental values.

Inspection of Table 1, shows that our best fit values are in disagreement with previous assignments in several respects. The reasons for some of these have already been discussed: the bands at 900 cm^{-1} were not considered to be fundamentals, the INS spectrum shows unambiguously that this is the case. Conversely, the bands around 1200 cm^{-1} assigned as fundamentals are not. This is seen in the INS spectrum and also in the infrared and Raman spectra calculated by CASTEP, see Figures 5 and 6 respectively. These only include fundamentals (since the calculation assumes the harmonic approximation and overtones and combinations result from anharmonicity) and there is no intensity at 1200 cm^{-1}.

Table 1. Mode description, symmetry and transition energies (cm^{-1}) for ruthenocene.

Description[a]	D_{5h} symmetry	Mode no.[b]	Adams [13]	Bodenheimer [14]	Prosenc [10a]	This work	
						CASTEP *P*nma	D_{5h} optimised
Torsion	A_1"	6	134	130	37		85
δ(ring–Ru–ring)	E_1'	22	168	170	438	160/168	167/177
ν(Ru–ring)	A_1'	4	333	333	322	323	335
ν(Ru–ring)	A_2"	11	450	380	375	373	389
Ring tilt	E_1"	16	400	400	373	382/387	400
Ring tilt	E_1'	21	381	450	147	441/446	455
π(CCC)	E_2'	28	604	603	577	595/598	595
π(CCC)	E_2"	34	604	600	570	583/586	602
π(C–H)	A_2"	9	808	808	791	789	808
π(C–H)	A_1'	2	818	818	803	814	818
δ(CCC)	E_2"	33	868	868	856	798/801	820
δ(CCC)	E_2'	27	902	900	823	825/829	838
π(C–H)	E_1"	14	839	842	794	805	840
π(C–H)	E_1'	19	829	834	784	837/845	866
π(C–H)	E_2"	31	1049	1050	821	882/888	904
π(C–H)	E_2'	25	1063	1065	866	894/900	904
δ(C–H)	E_1'	18	1000	1025	990	990/995	994
δ(C–H)	$E1$"	13	1001	1000	979	982/986	1007
δ(C–H)	E_2'	24	1187	1205	1043	1043/1056	1053
δ(C–H)	E_2"	30	1206	1188	1033	1037/1040	1064
ν(C–C)	A_1'	3	1099	1100	1093	1092	1100
ν(C–C)	A_2"	10	1099	1095	1096	1094	1100
δ(C–H)	A_2'	7	1251	1250	1235	1244	1253
δ(C–H)	A_1"	5	1251	1255	1234	1236	1253
ν(C–C)	E_2"	32	1342	1360	1330	1323/1330	1327
ν(C–C)	E_2'	26	1361	1360	1352	1344/1352	1341
ν(C–C)	E_1'	20	1406	1410	1394	1398/1399	1411
ν(C–C)	E_1"	15	1410	1410	1394	1389/1394	1411
ν(C–H)	E_1"	12	3080	3084	3162	3159/3164	3080
ν(C–H)	E_1'	17	3080	3076	3162	3164/3168	3080
ν(C–H)	E_2"	29	3095	3092	3147	3138/3139	3095
ν(C–H)	A_2"	8	3100	3100	3173	3170	3100
ν(C–H)	E_2'	23	3105	3104	3148	3170	3105
ν(C–H)	A_1'	1	3111	3112	3172	3176	3111

[a]ν = stretch, δ = in-plane bend, π = out-of-plane bend

[b]The mode numbering is that used by refs. [11] and [12].

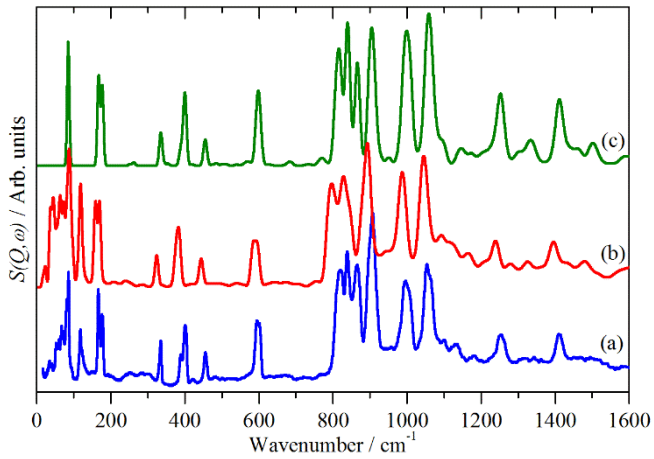

Figure 4. Comparison of INS spectra of ruthenocene: (a) experimental and those calculated by periodic-DFT calculation of the complete unit cell (b) and (c) after scaling the transition energies.

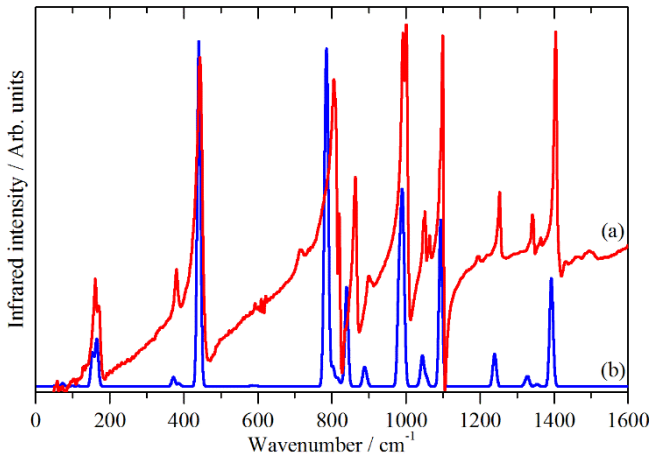

Figure 5. Comparison of infrared spectra of ruthenocene: (a) experimental and (b) calculated by periodic-DFT calculation of the complete unit. The derivative-like linehape in (a) is a particle size effect.

The most contentious assignments are for the metal–ring vibrations. There are five of these: symmetric and asymmetric (with respect to the horizontal mirror plane in the isolated molecule) Ru–ring stretch (ν_4, A_1' and ν_{11}, A_2") and Ru–ring tilt (ν_{16}, E_1" and ν_{21}, E_1') and the ring–Ru–ring bend (ν_{22}, E_1'). The symmetric Ru–ring stretch (ν_4, A_1') at 335 cm^{-1} is unambiguously assigned by its polarization characteristics in both solution and the solid.[13] It has been claimed[10a] that the Ru–ring tilt (ν_{21}, E_1') and the ring–Ru–ring bend (ν_{22}, E_1') are so mixed that the distinction between them is arbitrary. This is not correct. The ring–Ru–ring bend mode involves predominantly changes in the C–Ru–C bond angles with little change in the Ru–C bond lengths

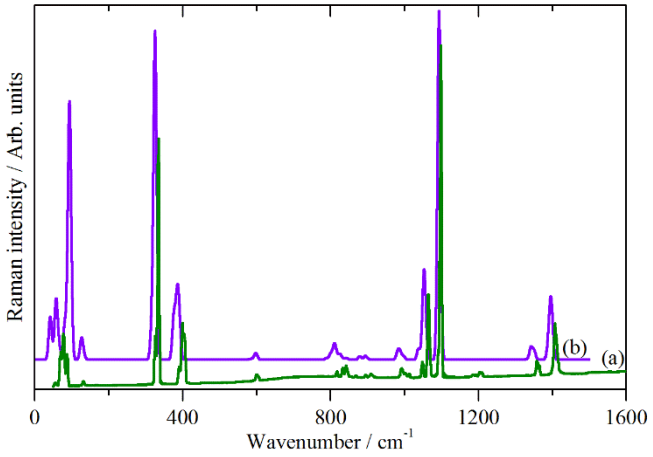

Figure 6. Comparison of Raman spectra of ruthenocene: (a) experimental and (b) calculated by periodic-DFT calculation of the complete unit.

and the reverse for the Ru–ring tilt mode. Inspection of the atomic displacements shows that for the mode at ~170 cm^{-1}, the C–Ru–C bond angles change by ± 3° with only a ± 0.01 Å change in the Ru–C bond length. While for the mode at ~450 cm^{-1}, the C–Ru–C bond angles change by <± 0.5° and the Ru–C bond length by ± 0.05 Å. Thus the 170 cm^{-1} mode must be the ring–Ru–ring bend (ν_{22}, E_1') and the 450 cm^{-1} mode the Ru–ring tilt (ν_{21}, E_1'). The other ambiguity has been between the asymmetric Ru–ring stretch (ν_{11}, A_2") and the Ru–ring tilt (ν_{21}, E_1'). Inspection of the mode visualizations confirms that the asymmetric Ru–ring stretch is at 389 cm^{-1} and, as previously discussed, that the Ru–ring tilt (ν_{21}, E_1') is at 450 cm^{-1}. This is also apparent from the simulation of the predicted spectra, Figure 3. We agree with the assignments of Bodenheimer and Low[14] in this region and it can be seen that Figure 3d is the only one that agrees with the experimental spectrum, Figure 3a.

The only remaining uncertainty is the location of the torsional mode. The mode visualizations show that the four factor group components are at 42, 58, 110 and 114 cm^{-1}, Table S1. The parent mode, ν_6, A_1" is infrared and Raman forbidden under D_{5h} symmetry, in the crystal it is allowed, but the induced activity is very small.

All previous work has implicitly used an isolated molecule model, whereby to satisfy the invariance of the center-of-mass of the system undergoing the motion (a condition for a normal mode), motion in one ring generates motion in the second ring. In the solid state, this requirement is more subtle: it is that the center-of-mass of the *unit cell* is invariant for an optic mode. Thus for a system that has more than one molecule in the primitive cell, such as ruthenocene (Z = 4), motion in one entity can be compensated by motion in another. For ruthenocene this means that only one ring of a molecule may be active in a given mode. Visualisation of the ~130 cm^{-1} mode, confirms that this is the case here and that it is a libration.

Conclusions

In this work we report a simplified synthesis of ruthenocene and we have also revisited the vibrational spectroscopy of this iconic molecule. The addition of INS data in combination with periodic-DFT calculations has enabled the first correct assignment of the internal modes of ruthenocene. By generating the INS spectra predicted by previous assignment schemes we are able to show that they all fail to correctly predict the experimental INS spectrum. This straightforward means to test proposed assignments is one of the great strengths of vibrational spectroscopy with neutrons.

Experimental Section

Materials: The synthesis of ruthenocene is described in the main text. Ruthenium trichloride hydrate was obtained from Johnson-Matthey and the zinc dust used was standard laboratory grade.

Vibrational spectroscopy: Variable temperature, 10 – 300 K, Raman spectra were recorded using 532 nm excitation with a modified Renishaw InVia system that has been previously described.[17] Infrared spectra were recorded using a Bruker Vertex70 FTIR spectrometer, over the range 100 to 4000 cm^{-1} at 4 cm^{-1} resolution with a DLaTGS detector using 64 scans and the Bruker Diamond ATR. The use of the ultra-wide range beamsplitter enabled the entire spectral range to be recorded without the need to change beamsplitters. The spectra have been corrected for the wavelength-dependent variation in path length using the Bruker software. The INS spectrum was recorded at <20 K using TOSCA[18] at ISIS.[19] The spectrum is available at the INS database: http://wwwisis2.isis.rl.ac.uk/INSdatabase/ .

Computational studies: The plane wave pseudopotential based program CASTEP was used for the calculation of the vibrational transition energies and their intensities.[20,21] Dispersion corrected density functional theory (DFT-D) calculations using the Tkatchenko and Scheffler[22] correction were carried out with the generalised gradient approximation (GGA) Perdew-Burke-Ernzerhof (PBE) functional in conjunction with optimised norm-conserving pseudopotentials. All of the calculations were converged to better than |0.0075| eV $Å^{-1}$. After geometry optimisation, the vibrational spectra were calculated in the harmonic approximation using density-functional perturbation-theory.[23] This procedure generates the vibrational eigenvalues and eigenvectors, which allows visualisation of the modes within Materials Studio[24] and is also the information needed to calculate the INS spectrum using the program ACLIMAX.[25] The initial structure for the optimisation was that determined at 100 K.[15c] This consistently resulted in one imaginary mode, irrespective of the convergence criteria used. Allowing both the lattice and the geometry to optimise resulted in a structure that was <1% larger (796.3 $Å^3$ *vs* 789.8 $Å^3$) and with no imaginary modes anywhere in the Brillouin zone, Figure S4. An isolated molecule calculation was generated by taking the optimised structure and removing three molecules from it. The eigenvectors from this were then used with the transition energies from Table 1 to generate Figures 3b,c,d and 4c.

Acknowledgements

The STFC Rutherford Appleton Laboratory is thanked for access to neutron beam facilities. Computing resources (time on the SCARF compute cluster for the CASTEP calculations) were provided by STFC's e-Science facility. Dr Dan Evans (Bangor University) is thanked for measuring the nmr spectra.

[1] a) T. J. Kealy, P. L. Pauson, *Nature*, **1951**, *168*, 1039; b) S. A. Miller, J. A. Tebboth J. F. Tremaine, *J . Chem. Soc. Resumed* **1952**, 632-635.
[2] G. Wilkinson, M. Rosenblum, M. C. Whiting, R. B. Woodward, *J. Amer. Chem. Soc.* **1952**, *74*, 2125-2126.
[3] G. Wilkinson, *J. Amer. Chem. Soc.* **1952**, *74*, 6146-6147.
[4] E. O. Fischer, H. Grumbert, *Chem. Ber.* **1959**, *92*, 2302-2309.
[5] B. V. Lokshin, V. T. Aleksanian, E. B. Rusach, *J. Organomet. Chem.* **1975**, *86*, 253-256.
[6] P. C. H. Mitchell, S. F. Parker, A. J. Ramirez-Cuesta, J. Tomkinson, *Vibrational spectroscopy with neutrons, with applications in chemistry, biology, materials science and catalysis*, World Scientific, Singapore, **2005.**
[7] S. F. Parker, D. Lennon. P.W. Albers, *Appl. Spec.* **2011**, *65*, 1325-1341.
[8] a) E. Kemner, I. M. de Schepper, G. J. Kearley, U. A. Jayasooriya, *J. Chem. Phys.* **2000**, *112*, 10926-10929; b) U. A. Jayasooriya, S. A. Malone, A. I. Chumakov,R. Rüffer, A. R. Overweg, C. R. Nicklin, *ChemPhysChem* **2001**, *2*, 177-180.
[9] D. E. Bublitz, W. E. McEwen, and J. Kleinberg, *Org. Synth.* **1961**, *41*, 96-99.
[10] a) M. H. Prosenc, H. Reddmann, H.-D. Amberger, *Spectrochimica Acta Part A*, **2012**, *87*, 126-134; b) C. Latouche, F. Palazzetti, D. Skouteris, V. Barone, *J. Chem. Theory Comput.* **2014**, *10*, 4565–4573.
[11] a) M. D. Rausch, E. O. Fischer, H. Grubert, *J. Amer. Chem. Soc.*,**1960**, *82*, 76-82. b) G.J. Gauthier, *J. Chem Soc., D: Chem. Comm.,* **1969,** *13*, 690. c) D. C. Liles, A. Shaver, E. Singleton, Eric; M. B., *J. Organomet. Chem.* **1985**, *288*, C33-C36.d) M. O. Albers, D.C, Liles, D.J. Robinson, A. Shaver,E. Singleton,M. B. Wiege, J. C. A. Boeyens, D.C. Levendis, *Organometallics*, **1986,** *5*, 2321-7.e) C. H. Winter, S. Pirzad, D, H, Cao, *J. Chem. Soc., Chem. Comm.*, **1991**, 1026-.7.
[12] a) P. Pertici, G. Vitulli,,L. Porri, *J. Chem. Soc., Chem. Comm,* **1975**, 846. b) A. Z. Rubezhov, A. S. Ivanov, A. A. Bezrukova, *Izv. Akad. Nauk SSSR, Ser. Khim.,* 1979, 1606-8.
[13] D. M. Adams, W. S. Fernando, *J. Chem. Soc. Dalton* **1972**, 2507-2511.
[14] J. S. Bodenheimer, W. Low, *Spectrochimica Acta Part A* **1973**, *29*, 1733-1743.
[15] a) G. L. Hardgrove, D. H. Templeton, *Acta Cryst.* **1959**, *12*, 28-32; b) P. Seiler, J. D. Dunitz, *Acta Cryst.* **1980**, *B36*, 2946-2950; c) A. O. Borissova, M. Yu. Antipin, D. S. Perekalin, K. A. Lyssenko, *CrystEngComm* **2008**, *10*, 827–832; d) Y Miyamoto, S. Takamizawa, *Dalton Trans.* **2015**, *44*, 5688–5691.
[16] J. Tomkinson, S. F. Parker, *Spectrochimica Acta Part A* **2011**, *79*, 2017-2019.
[17] M. A. Adams, S.F. Parker, F. Fernandez-Alonso, D.J. Cutler, C. Hodges, A. King, *Appl. Spec.* **2009**, *63*, 727-732.
[18] S. F. Parker, F. Fernandez-Alonso, A. J. Ramirez-Cuesta, J. Tomkinson, S. Rudic, R. S. Pinna, G. Gorini, J. Fernández Castañon, *J. Phys. Conf. Series* **2014**, *554*, 012003.
[19] http://www.isis.stfc.ac.uk/
[20] S. J. Clark, M. D. Segall, C. J. Pickard, P. J. Hasnip, M. J. Probert, K. Refson, M. C. Payne, *Z. Kristallographie* **2005**, *220*, 567-570.
[21] K. Refson, S. J. Clark, P. R. Tulip, *Phys. Rev. B* **2006**, *73*, 155114.
[22] A. Tkatchenko and M. Scheffler, *Phys. Rev. Lett.* **2009**, *102*, 073005.
[23] V. Milman, A. Perlov, K. Refson, S. J. Clark, J. Gavartin, B. Winkler. *J. Phys.: Condens. Matter* **2009**, *21*, 485404.
[24] http://accelrys.com/products/collaborative-science/biovia-materials-studio/
[25] A. J. Ramirez-Cuesta, *Comp. Phys. Comm.* **2004**, *157*, 226-238.

SUPPORTING INFORMATION

Title: Synthesis and inelastic neutron scattering spectroscopy of ruthenocene
Author(s): Stewart F. Parker,* and Ian R. Butler

Contents **Page**

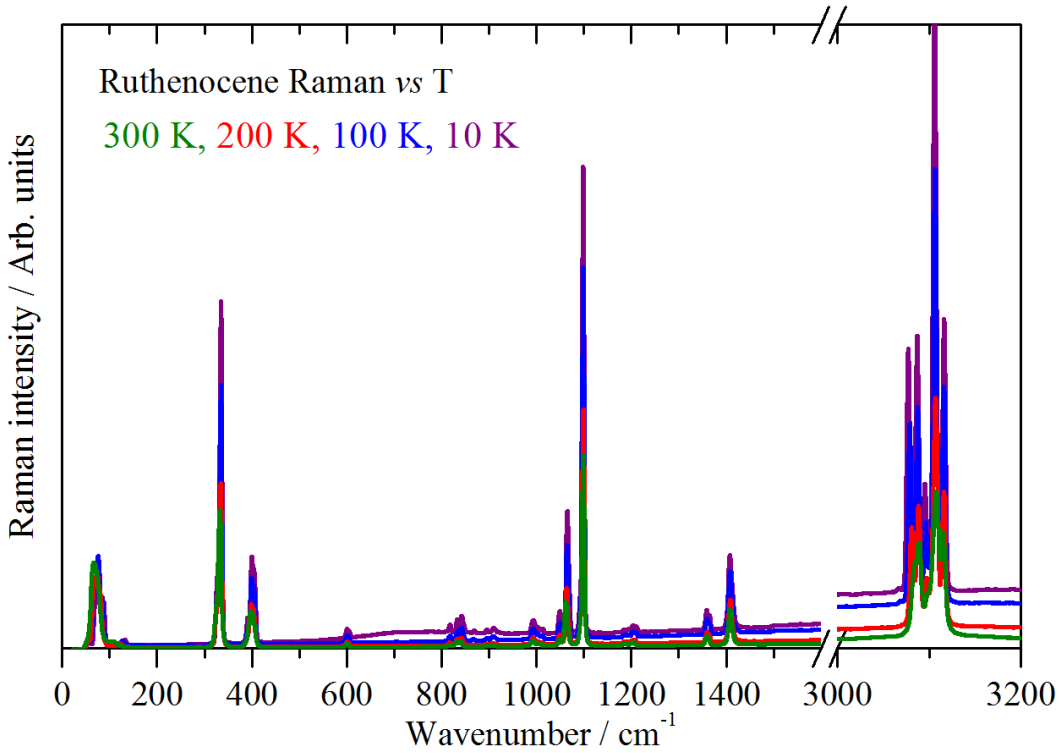

Figure S1. Variable temperature 532 nm Raman spectra of ruthenocene.

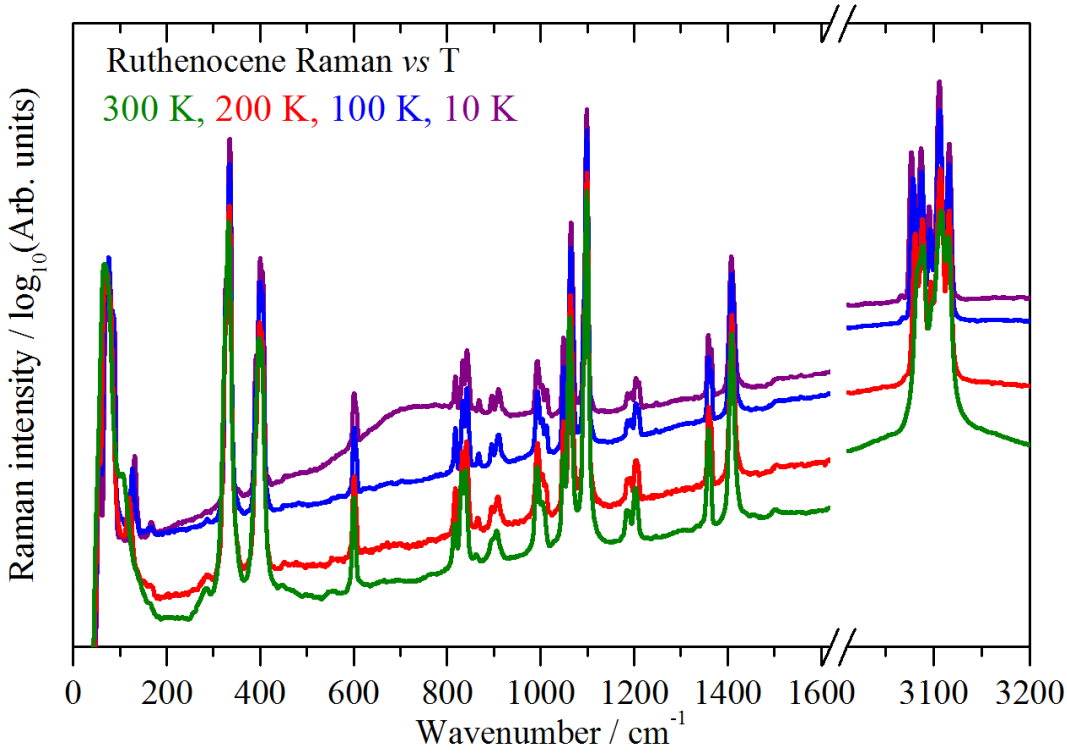

Figure S2. Variable temperature 532 nm Raman spectra of ruthenocene. Same data as Figure S1, but with the *y*-axis on a logarithmic scale.

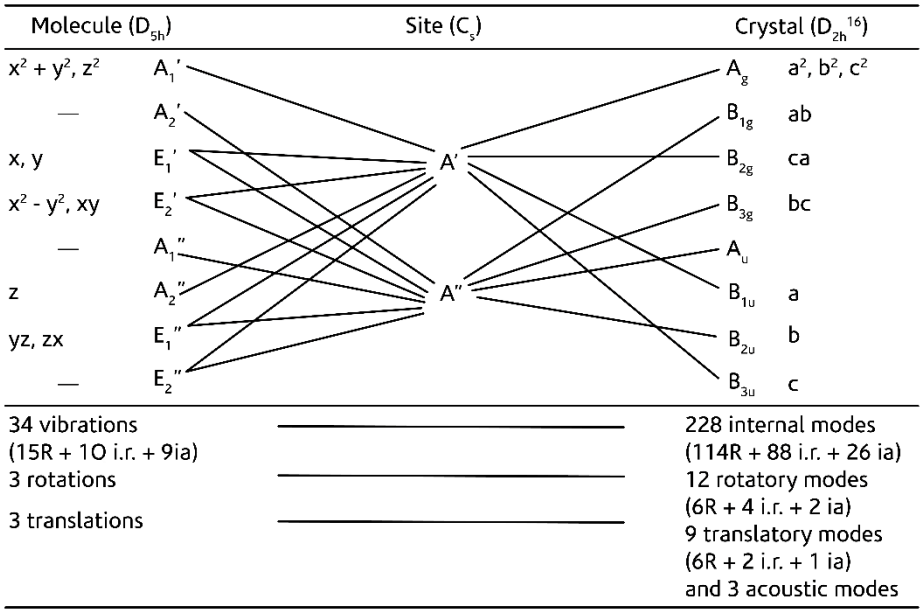

Figure S3. Correlation scheme for ruthenocene. Reproduced from: J. S. Bodenheimer, W. Low, *Spectrochimica Acta Part A* **1973**, *29*, 1733-1743, with permission of Elsevier.

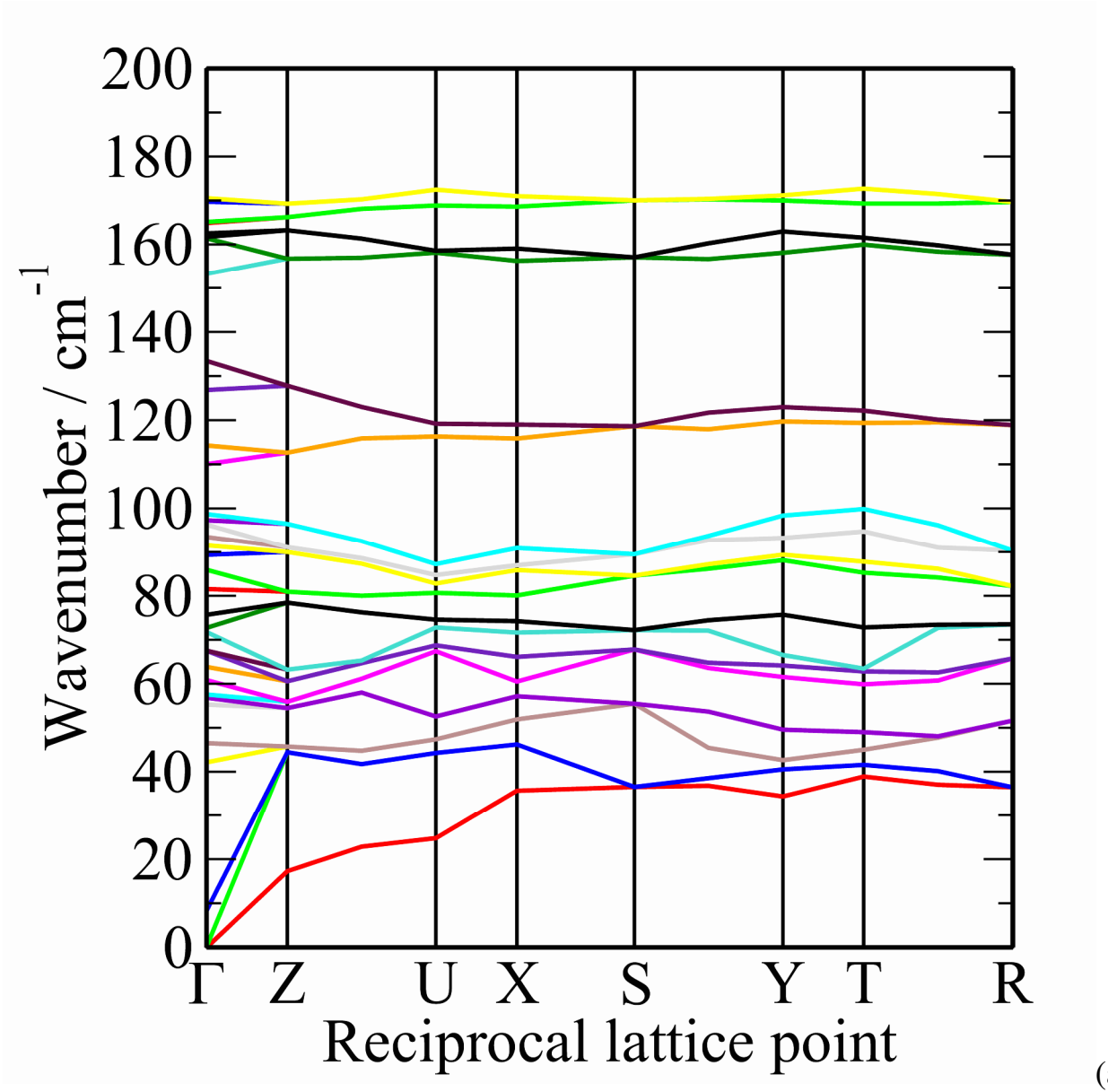
200
180
160
140
120
100
80
60
40
20
0
Wavenumber / cm-1
Γ
Z
U
X
S
Y
T
R
Reciprocal lattice point

(a)

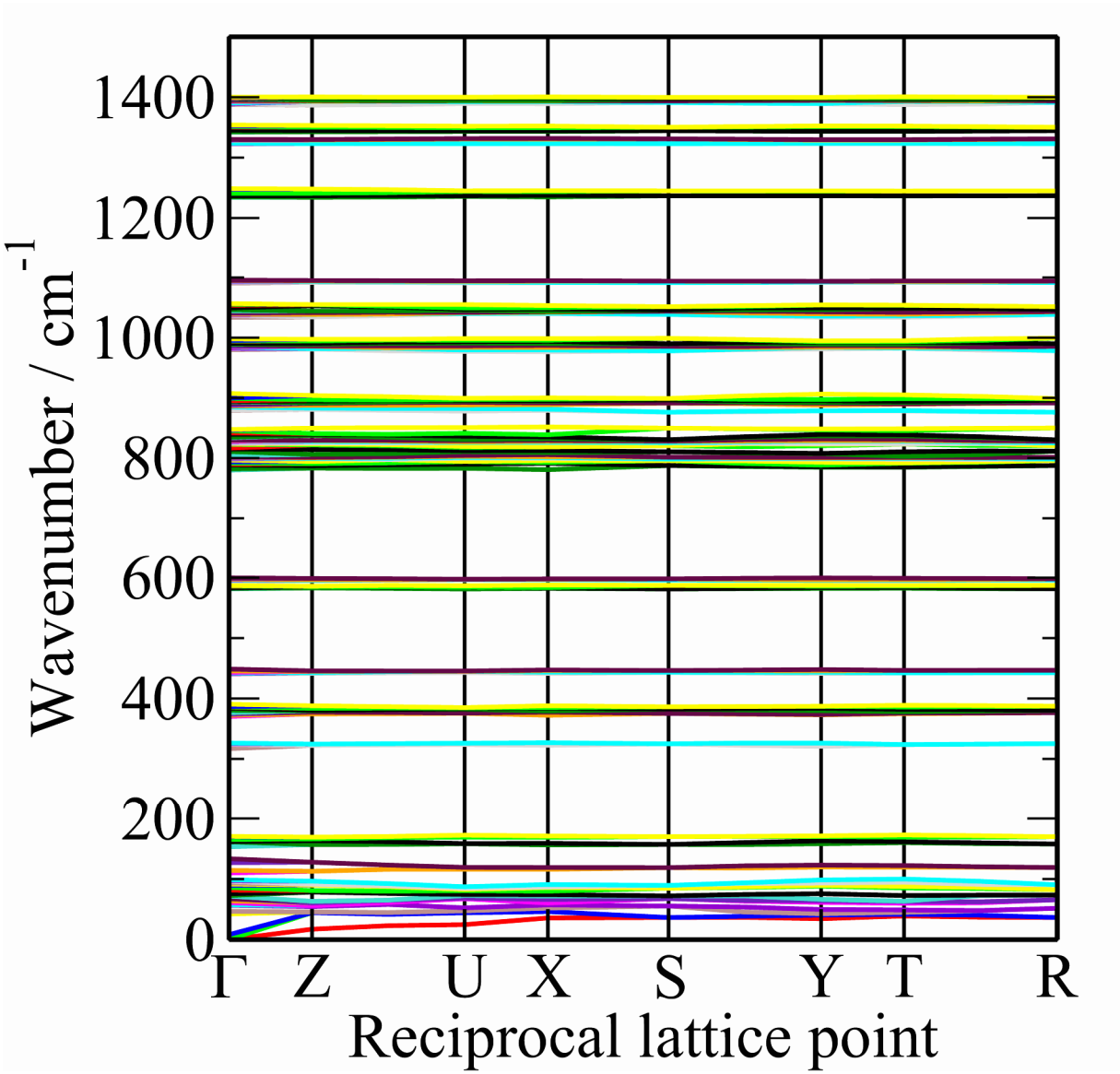
1400
1200
1000
800
600
400
200
0
Wavenumber / cm-1
Γ
Z
U
X
S
Y
T
R
Reciprocal lattice point

(b)

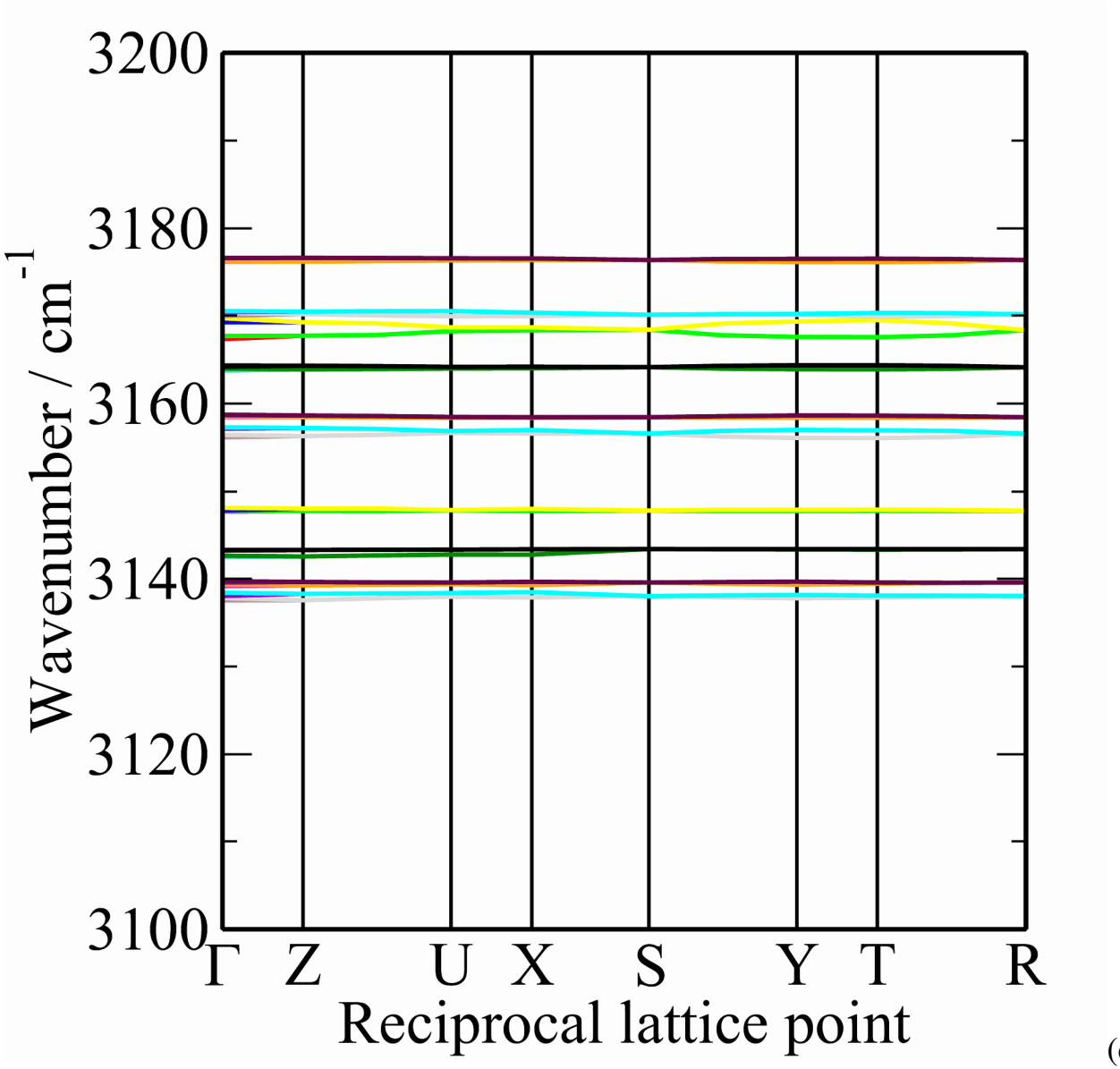

(c)

Figure S4. Dispersion curves for ruthenocene generated from the lattice and geometry optimised *P*nma structure. (a) 0 – 200 cm^{-1}, (a) 0 – 1500 cm^{-1}, and (a) 3100 – 3200 cm^{-1}. Note the absence of imaginary (negative frequency) modes.

Table S1. Calculated transition energies, mode number, symmetries and infrared and Raman intensities for ruthenocene in the lattice and geometry optimised *P*nma structure.

Transition energy / cm^{-1}	*P*nma symmetry	Mode number for D_{5h} structure	D_{5h} symmetry	Infrared intensity / (Debye $Å^{-1})^2(amu)^{-1}$	Raman intensity / $Å^4 (amu)^{-1}$
0	B3u			0.00	0.00
0	B1u			0.00	0.00
0	B2u			0.00	0.00
8	Au			0.00	0.00
42	B1g	6	A2" torsion	0.00	2.87
47	B2u		? Single ring tors	0.00	0.00
55	B1u		a trans	0.03	0.00
57	Au		C2 Lib	0.00	0.00
58	B3g	6	A2"torsion	0.00	6.82
61	B2g		c trans	0.00	0.20
64	B3g		b trans or lib?	0.00	1.13
67	B1g		b trans or lib?	0.00	0.34
68	Ag		c trans	0.00	0.64
72	B3u		c trans	0.00	0.00
73	B2u		? Single ring tors	0.10	0.00
76	Au		? Single ring tors	0.00	0.00
82	Ag		c trans	0.00	8.03
86	B2g		a trans	0.00	0.00
89	B1u		C2 Lib	0.00	0.00
92	B3g		? Single ring tors	0.00	6.33
93	Ag		C2 Lib	0.00	50.43
96	B2g		C2 Lib	0.00	19.30
97	B1g		? Single ring tors	0.00	6.13
99	B3u		C2 Lib	0.02	0.00
110	Au	6	A2" torsion	0.00	0.00
114	B2u	6	A2" torsion	0.02	0.00
127	B3g		C5 Lib	0.00	10.79
133	B1g		C5 Lib	0.00	1.49
153	B3u	21	E1'	1.18	0.00
161	Ag	21	E1'	0.00	0.27
162	B1u	21	E1'	0.07	0.00
163	B2g	21	E1'	0.00	0.00
165	Au	21	E1'	0.00	0.00
165	B2u	21	E1'	1.66	0.00
170	B3g	21	E1'	0.00	0.01

171	B1g	21	E1'	0.00	0.00
317	B2g	4	A1'	0.00	68.59
324	B1u	4	A1'	0.00	0.00
326	Ag	4	A1'	0.00	725.44
326	B3u	4	A1'	0.00	0.00
370	B3u	11	A2"	0.01	0.00
372	B1u	11	A2"	0.30	0.00
374	Au	11	A2"	0.00	0.00
376	B3u	11	A2"	0.03	0.00
376	Ag	16	E1"	0.00	107.86
381	B2g	16	E1"	0.00	9.86
384	Ag	16	E1"	0.00	58.36
385	B1u	16	E1"	0.01	0.00
385	B1g	16	E1"	0.00	36.15
386	B2g	16	E1"	0.00	50.96
387	B2u	16	E1"	0.10	0.00
390	B3g	16	E1"	0.00	107.23
440	B3u	22	E1'	4.92	0.00
440	B2u	22	E1'	6.18	0.00
441	Ag	22	E1'	0.00	0.30
442	B3g	22	E1'	0.00	0.04
443	Au	22	E1'	0.00	0.00
444	B1u	22	E1'	1.98	0.00
448	B2g	22	E1'	0.00	0.20
449	B1g	22	E1'	0.00	0.16
582	B2g	34	E2"	0.00	0.02
582	Ag	34	E2"	0.00	3.20
583	B2u	34	E2"	0.02	0.00
585	B1u	34	E2"	0.00	0.00
586	Au	34	E2"	0.00	0.00
586	B3g	34	E2"	0.00	0.93
587	B1g	34	E2"	0.00	0.87
587	B3u	34	E2"	0.01	0.00
594	B3u	28	E2'	0.00	0.00
594	B1u	28	E2'	0.01	0.00
595	B1g	28	E2'	0.00	0.82
596	B2g	28	E2'	0.00	9.65
597	Ag	28	E2'	0.00	7.94
597	B2u	28	E2'	0.01	0.00
599	Au	28	E2'	0.00	0.00
600	B3g	28	E2'	0.00	16.78
780	B3u	14	E1"	0.31	0.00
781	B1u	14	E1"	4.44	0.00
786	B1u	9	A2"	9.11	0.00
788	Ag	9	A2"	0.00	7.25
789	B2g	9	A2"	0.00	2.02
790	B3u	9	A2"	1.21	0.00
794	Au	14	E1"	0.00	0.00

797	B2u	33	E2"	0.02	0.00
798	B3u	33	E2"	0.10	0.00
799	B2g	33	E2"	0.00	5.06
800	Au	33	E2"	0.00	0.00
800	Ag	33	E2"	0.00	26.55
801	B1g	33	E2"	0.00	1.04
801	B3g	33	E2"	0.00	2.70
802	B2u	14	E1"	0.18	0.00
803	Ag	14	E1"	0.00	9.87
804	B1u	33	E2"	0.49	0.00
811	B2g	2	A1'	0.00	102.59
815	B3u	2	A1'	0.30	0.00
815	B1u	2	A1'	0.00	0.00
816	Ag	2	A1'	0.00	18.04
823	B1g	14	E1"	0.00	0.50
823	B3u	27	E2'	0.02	0.00
823	B2g	27	E2'	0.00	0.69
824	B3g	14	E1"	0.00	21.07
825	Ag	27	E2'	0.00	8.46
827	B1g	27	E2'	0.00	2.59
828	B1u	27	E2'	0.09	0.00
828	B3g	27	E2'	0.00	2.54
829	B2u	27	E2'	0.03	0.00
830	Au	27	E2'	0.00	0.00
830	B2g	14	E1"	0.00	9.23
834	B3u	19	E1'	0.00	0.00
835	B3g	19	E1'	0.00	1.03
840	Ag	19	E1'	0.00	0.54
840	B1u	19	E1'	3.61	0.00
842	B2g	19	E1'	0.00	8.24
845	B1g	19	E1'	0.00	3.72
846	B2u	19	E1'	0.00	0.00
847	Au	19	E1'	0.00	0.00
879	Ag	31	E2"	0.00	24.18
879	B2g	31	E2"	0.00	0.32
885	B1g	31	E2"	0.00	0.17
885	B3g	31	E2"	0.00	2.95
886	B3u	25	E2'	0.13	0.00
886	B2u	31	E2"	0.20	0.00
888	B1u	31	E2"	0.21	0.00
891	B3u	31	E2"	0.17	0.00
894	Au	31	E2"	0.00	0.00
894	B2u	25	E2'	0.16	0.00
894	B1g	25	E2'	0.00	23.06
895	B1u	25	E2'	0.00	0.00
895	Ag	25	E2'	0.00	5.22
899	Au	25	E2'	0.00	0.00
900	B2g	25	E2'	0.00	1.71

907	B3g	25	E2'	0.00	2.19
980	Ag	13	E1"	0.00	15.16
981	B2u	13	E1"	3.79	0.00
982	B1g	13	E1"	0.00	36.14
984	B2g	13	E1"	0.00	19.58
984	Au	18	E1'	0.00	0.00
985	B1u	13	E1"	0.06	0.00
985	B3u	13	E1"	0.04	0.00
988	B3g	13	E1"	0.00	28.65
989	B3g	18	E1'	0.00	25.67
989	B3u	18	E1'	4.38	0.00
990	Au	13	E1"	0.00	0.00
992	B1u	18	E1'	1.42	0.00
994	B1g	18	E1'	0.00	0.00
994	B2u	18	E1'	1.84	0.00
995	B2g	18	E1'	0.00	4.96
998	Ag	18	E1'	0.00	25.33
1034	B3g	30	E2"	0.00	0.06
1037	B2u	30	E2"	0.10	0.00
1038	B2g	30	E2"	0.00	66.75
1039	B1g	30	E2"	0.00	0.00
1039	Ag	30	E2"	0.00	32.31
1039	B3u	30	E2"	0.00	0.00
1040	Au	30	E2"	0.00	0.00
1042	Au	24	E2'	0.00	0.00
1044	B1u	30	E2"	0.97	0.00
1046	B2u	24	E2'	0.08	0.00
1049	B1u	24	E2'	0.12	0.00
1052	B1g	24	E2'	0.00	424.93
1054	Ag	24	E2'	0.00	284.20
1055	B3u	24	E2'	0.30	0.00
1056	B3g	24	E2'	0.00	105.66
1057	B2g	24	E2'	0.00	71.69
1091	B3u	3	A1'	0.21	0.00
1092	B1u	3	A1'	0.67	0.00
1093	Ag	3	A1'	0.00	911.81
1093	B2g	3	A1'	0.00	9.66
1094	B1u	10	A2"	4.22	0.00
1094	Ag	10	A2"	0.00	2382.24
1095	B2g	10	A2"	0.00	13.36
1095	B3u	10	A2"	1.14	0.00
1234	B1g	5	A1"	0.00	3.85
1235	B3g	5	A1"	0.00	0.32
1237	Au	5	A1"	0.00	0.00
1237	B2u	5	A1"	0.50	0.00
1241	Au	7	A2'	0.00	0.00
1241	B2u	7	A2'	0.81	0.00
1247	B3g	7	A2'	0.00	0.65

1248	B1g	7	A2'	0.00	0.28
1323	B2u	32	E2"	0.14	0.00
1323	Au	32	E2"	0.00	0.00
1323	B3g	32	E2"	0.00	0.02
1324	B1g	32	E2"	0.00	0.02
1329	B2g	32	E2"	0.00	1.80
1329	B1u	32	E2"	0.32	0.00
1330	B3u	32	E2"	0.00	0.00
1330	Ag	32	E2"	0.00	4.28
1342	B1g	26	E2'	0.00	113.62
1342	B3g	26	E2'	0.00	26.16
1345	B2u	26	E2'	0.00	0.00
1345	Au	26	E2'	0.00	0.00
1350	B2g	26	E2'	0.00	31.27
1351	Ag	26	E2'	0.00	71.84
1352	B1u	26	E2'	0.00	0.00
1354	B3u	26	E2'	0.08	0.00
1388	B1g	15	E1"	0.00	73.94
1389	B3g	15	E1"	0.00	20.29
1389	Au	15	E1"	0.00	0.00
1390	B2u	15	E1"	1.39	0.00
1393	B3u	15	E1"	1.80	0.00
1394	Ag	15	E1"	0.00	398.19
1394	B1u	15	E1"	0.94	0.00
1395	B2g	15	E1"	0.00	74.90
1398	B2u	20	E1'	0.04	0.00
1398	B1u	20	E1'	0.16	0.00
1398	B3g	20	E1'	0.00	208.88
1398	B3u	20	E1'	0.03	0.00
1398	Au	20	E1'	0.00	0.00
1399	Ag	20	E1'	0.00	91.69
1399	B1g	20	E1'	0.00	45.27
1400	B2g	20	E1'	0.00	48.18
3138	B1u	29	E2"	0.16	0.00
3138	B3u	29	E2"	0.83	0.00
3138	B2g	29	E2"	0.00	16.51
3138	Ag	29	E2"	0.00	1763.99
3139	Au	29	E2"	0.00	0.00
3139	B3g	29	E2"	0.00	8.13
3140	B2u	29	E2"	0.07	0.00
3140	B1g	29	E2"	0.00	1149.73
3143	B2u	23	E2'	2.51	0.00
3143	Au	23	E2'	0.00	0.00
3143	B1g	23	E2'	0.00	2459.38
3143	B3g	23	E2'	0.00	360.10
3148	B3u	23	E2'	0.00	0.00
3148	B1u	23	E2'	0.24	0.00
3148	B2g	23	E2'	0.00	324.91

3148	Ag	23	E2'	0.00	844.67
3156	Ag	12	E1"	0.00	2913.73
3156	B3u	12	E1"	0.01	0.00
3157	B1u	12	E1"	0.18	0.00
3157	B2g	12	E1"	0.00	142.52
3158	Au	12	E1"	0.00	0.00
3159	B3g	12	E1"	0.00	792.09
3159	B2u	12	E1"	0.00	0.00
3159	B1g	12	E1"	0.00	4.84
3164	B2u	17	E1'	0.09	0.00
3164	B1g	17	E1'	0.00	294.43
3164	Au	17	E1'	0.00	0.00
3164	B3g	17	E1'	0.00	230.60
3167	B2g	17	E1'	0.00	1022.87
3168	B1u	17	E1'	1.17	0.00
3169	Ag	17	E1'	0.00	6598.43
3170	B3u	17	E1'	0.17	0.00
3170	B3u	8	A2"	0.06	0.00
3170	B2g	8	A2"	0.00	8.34
3170	B1u	8	A2"	0.00	0.00
3171	Ag	8	A2"	0.00	2468.22
3176	B3u	1	A1'	0.04	0.00
3176	Ag	1	A1'	0.00	5582.12
3177	B1u	1	A1'	0.15	0.00
3177	B2g	1	A1'	0.00	933.39